Analytical formulations for annular disk sound radiation using structural modes

Ming-ran Lee and Rajendra Singh
Acoustics and Dynamics Laboratory, Department of Mechanical Engineering, The Ohio State University, Columbus, Ohio 43210-1107

(Received 10 May 1993; revised 3 January 1994; accepted 25 February 1994)

Sound radiation characteristics of an annular disk with application to the computer disk are examined analytically. The far-field and the radiation impedance approaches are employed to calculate radiated sound of a disk vibrating at its elastic or rigid body modes. Modal sound power is formulated by approximating the structural modal functions and is expressed in terms of a power series of the wave number. Predictions show that axisymmetric vibration modes are more efficient radiators compared to those asymmetric disk modes that have the same number of nodal circles. Numerical results obtained by a boundary element program are used to support analytical predictions. Formulations are also extended to include the modal coupling and source rotation effects. The effect of coupling between disk vibration modes on the radiated sound is found to be significant if multimodes are excited. A simple empirical equation has been developed to predict the modal sound radiation efficiency of a rotating disk for selected vibration modes.

PACS numbers: 43.40.Dx, 43.40.Rj

INTRODUCTION

A fundamental knowledge of sound radiation characteristics of annular/circular disks and the like radiators is necessary from machinery noise control and electroacoustic transducer design viewpoints. Obviously the classical case is the piston radiator, which is essentially a circular disk vibrating in the rigid body translating mode.[1-8] Only a few studies have dealt with sound radiation characteristics of a clamped circular disk vibrating at its elastic modes by using empirical[9] or numerical[10] approaches; others formulated analytically for specific asymptotic cases.[11] However, virtually no attention has been focused on the sound radiation from an annular disk vibrating at its flexure. Specifically, key issues such as the modal radiation characteristics of stationary and rotating disks and the acoustic coupling effects associated with multimodal excitation are yet to be examined. This study attempts to fill this void by developing new sound radiation efficiency formulations of an annular disk for both elastic deformation and rigid body modes. Relevant literature[1-28] will be discussed further in each main section. The example case, as shown in Fig. 1, is motivated by the computer hard disk (3.5-in.) drive noise problem. The problem will be formulated in a generic manner with potential applications to geared systems, circular saws, transducers, etc. It is assumed that a single annular disk radiates sound into a hemispherical free field as shown in Fig. 1. Fluid loading effects are ignored since air is the medium and the frequency range of interest for the sample case is up to 10 kHz.

I. STRUCTURAL MODAL CHARACTERISTICS

A. Exact and approximate solutions of a stationary disk

Natural frequencies ω_{mn} of an annular disk for the transverse flexural motion $w(r,\varphi,t)$ are determined by applying the classical thin plate theory,[29] where m and n denote the number of nodal circles and diameters, respectively. The governing equation of plate flexure is

$$D\left(\frac{\partial^2}{\partial r^2}+\frac{1}{r}\frac{\partial}{\partial r}+\frac{1}{r^2}\frac{\partial^2}{\partial \varphi^2}\right)^2 w+\rho h\frac{\partial^2 w}{\partial t^2}=F(r,\varphi,t), \quad (1a)$$

$$D=Eh^3/12(1-\nu^2). \quad (1b)$$

E is the Young's modulus, h is the plate thickness, ν is Poisson's ratio, ρ is the density, and F is the excitation function.

For a stationary disk, the compression exerted by the collars essentially simulates the clamped boundary condition at the inner edge ($r=a$), which is expressed as

$$w=0, \quad (2)$$

$$\frac{\partial w}{\partial r}=0. \quad (3)$$

Since the outer edge ($r=b$) is free, it is defined by

$$\frac{\partial^2 w}{\partial r^2}+\nu\left(\frac{1}{r}\frac{\partial w}{\partial r}+\frac{1}{r^2}\frac{\partial^2 w}{\partial \varphi^2}\right)=0, \quad (4)$$

$$\frac{\partial}{\partial r}\left(\frac{\partial^2 w}{\partial r^2}+\frac{1}{r}\frac{\partial w}{\partial r}+\frac{1}{r^2}\frac{\partial^2 w}{\partial \varphi^2}\right)+\frac{1-\nu}{r^2}\frac{\partial^2}{\partial \varphi^2}\left(\frac{\partial w}{\partial r}-\frac{w}{r}\right)=0. \quad (5)$$

 0001-4966/94/95(6)/3311/13/$6.00 © 1994 Acoustical Society of America

Singh-068

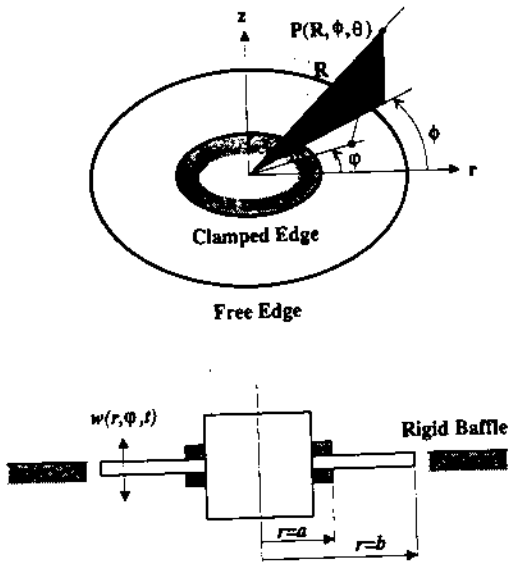

FIG. 1. Schematic of the computer disk radiating sound into a hemispherical free field.

The eigensolution consists of various Bessel functions and is expressed by[29]

$$\psi_{mn}(r,\varphi,t)=e^{j\omega_{mn}t}\cos(n\varphi)\,[c_1J_n(\beta_{mn}r)+c_2Y_n(\beta_{mn}r)+c_3I_n(\beta_{mn}r)+c_4K_n(\beta_{mn}r)], \tag{6a}$$

$$\beta_{mn}=\sqrt[4]{\omega_{mn}^2\rho h/D}. \tag{6b}$$

The vibration modes and natural frequencies are determined by solving the characteristic equation, which is obtained by substituting Eq. (6) into Eqs. (2)–(5). Since the exact solutions of vibration modes are expressed in terms of the Bessel functions, it is very complicated, if not impossible, to derive an analytical formulation expression for the radiation efficiency. Therefore, a polynomial approximation for the natural mode ψ_{mn} is employed here to avoid this problem. The approximate modal function consists of admissible or trial functions that satisfy the geometric boundary conditions at $r=a$ and is given by

$$\psi_{mn}(r,\varphi)=\cos(n\varphi)\sum_{s=2}^{N(m)}c_{mn,s}(r-a)^s. \tag{7}$$

The number of trial functions N is decided by the modal index m. In this study, the highest term of polynomial N is assigned to be 8. The potential energy (PE) and the kinetic energy (KE) are obtained by substituting the approximate modal function into the following equations:[30]

$$\mathrm{PE}=\frac{D}{2}\int_0^{2\pi}\int_a^b\left((\nabla^2\psi_{mn})^2-2(1-\nu)\times\left\{\frac{\partial^2\psi_{mn}}{\partial r^2}\left(\frac{1}{r}\frac{\partial\psi_{mn}}{\partial r}+\frac{1}{r^2}\frac{\partial^2\psi_{mn}}{\partial\varphi^2}\right)-\left[\frac{\partial}{\partial r}\left(\frac{1}{r}\frac{\partial\psi_{mn}}{\partial\varphi}\right)\right]^2\right\}\right)r\,dr\,d\varphi, \tag{8}$$

TABLE I. Dimensions and material properties of the sample computer disk.

Property	Dimension
Outer radius b (m)	$47.5E-3$
Inner radius a (m)	$16.0E-3$
Thickness h (m)	$0.81E-3$
Density ρ (kg/m^3)	$2.8E3$
Young's modulus E (N/m^2)	$6.19E10$
Poisson's ratio ν	0.3

$$\mathrm{KE}=\frac{\rho h}{2}\int_0^{2\pi}\int_a^b\left(\frac{\partial\psi_{mn}}{\partial t}\right)^2 r\,dr\,d\varphi. \tag{9}$$

The following set of linear equations is then obtained by applying the energy principle:[29–31]

$$\begin{bmatrix}\Lambda_{22}&\Lambda_{23}&\cdots&\Lambda_{2N}\\ \Lambda_{32}&\Lambda_{33}&\cdots&\Lambda_{3N}\\ \vdots&\vdots&\ddots&\vdots\\ \Lambda_{N2}&\Lambda_{N3}&\cdots&\Lambda_{NN}\end{bmatrix}\begin{bmatrix}c_{mn,2}\\ c_{mn,3}\\ \vdots\\ c_{mn,N}\end{bmatrix}=\begin{bmatrix}0\\0\\ \vdots\\0\end{bmatrix}, \tag{10a}$$

where

$$\Lambda_{ij}=ij(i-1)(j-1)X_1^{i+j-4}+\nu ij(i+j-2)X_0^{i+j-3}+\{ij[2(1-\nu)n^2+1]-\nu n^2(i^2+j^2-i-j)\}\times X_{-1}^{i+j-2}-(3-2\nu)n^2(i+j)X_{-2}^{i+j-1}+n^2[n^2+2(1-\nu)]X_{-3}^{i+j}-\beta_{mn}X_1^{i+j}, \tag{10b}$$

$$X_k^l=\int_a^b(r-a)^l r^k\,dr=\begin{cases}\dfrac{(b-a)^{l+1}}{l+1}, & k=0,\\ (b-a)^{l+1}\left(\dfrac{b-a}{l+2}+\dfrac{a}{l+1}\right), & k=1,\\ \dfrac{l!(-a)^{l+k+1}}{(l+k+1)!(-k-1)}\log\left(\dfrac{b}{a}\right)\end{cases}+\sum_{s=0,s\neq l+k+1}^{l}\frac{l!(-a)^s(b^{l+k-s+1}-a^{l+k-s+1})}{(l+k-s+1)(l-s)!s!},\quad k<0. \tag{10c}$$

Equation (10) yields the approximate natural frequencies and the coefficients of associated modal trial functions defined by Eq. (7).

B. Experimental results and analytical predictions

A 3.5-in. computer hard disk whose dimensions and material properties are listed in Table I is used as the sample case. Impact modal testing on a stationary disk has been conducted to validate the analytical results. A single computer disk is mounted on a rigid shaft between the spacing collars, which are used in the disk drive in order to simulate the real boundary conditions. The Young's mod-

TABLE II. Selected natural frequencies of the sample disk.[a]

Case	(m,n)	$\omega_{mn}/2\pi$ (Hz)			
		(0,2)	(0,0)	(0,3)	(0,1)
Free–free	Experiment	408	682	997	1530
	Prediction	408	682	1000	1530
Case	(m,n)	(0,1)	(0,2)	(0,3)	(0,4)
Clamped–free	Experiment	613	711	1130	1840
	Prediction	602	713	1120	1820

[a] (m,n) = (number of nodal circles, number of nodal diameters).

ulus is estimated by comparing the predicted first natural frequency of a free–free disk with the experiment result. Analytical predictions of natural frequencies match the measured values as shown in Table II. The approximate polynomial mode shapes and exact solutions for two axisymmetric modes of the sample disk are shown in Fig. 2. Excellent agreement is evident. Additionally, selected mode shapes obtained from the approximated modal functions are illustrated in Fig. 3. It is observed that there is a weak coupling between radial and circumferential modes and hence further simplification is possible.

II. MODAL RADIATION EFFICIENCY FORMULATIONS

Sound power radiated from a planar radiator is typically calculated by employing two approaches: the far-field sound pressure expression and the surface/near-field intensity expression.[13] The first approach essentially integrates the far-field Green's function over the surface of a radiator. The second approach usually transforms the time domain problem into the wave number domain. The task of finding the sound power then becomes how to evaluate adequately

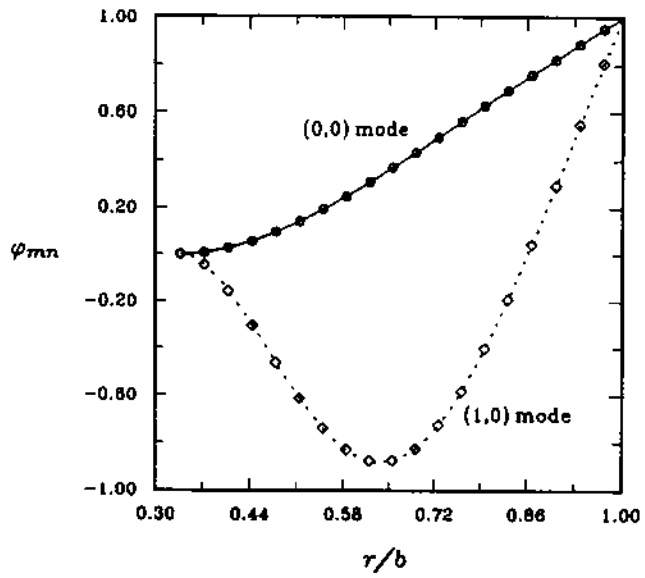

FIG. 2. Comparison between approximated and exact vibration modes of a 3.5-in. computer disk: empty symbols: exact solution; solid line: polynomial approximation. Key: ——— and ○○○○, (0,0) mode; ----- and □□□□, (1,0) mode.

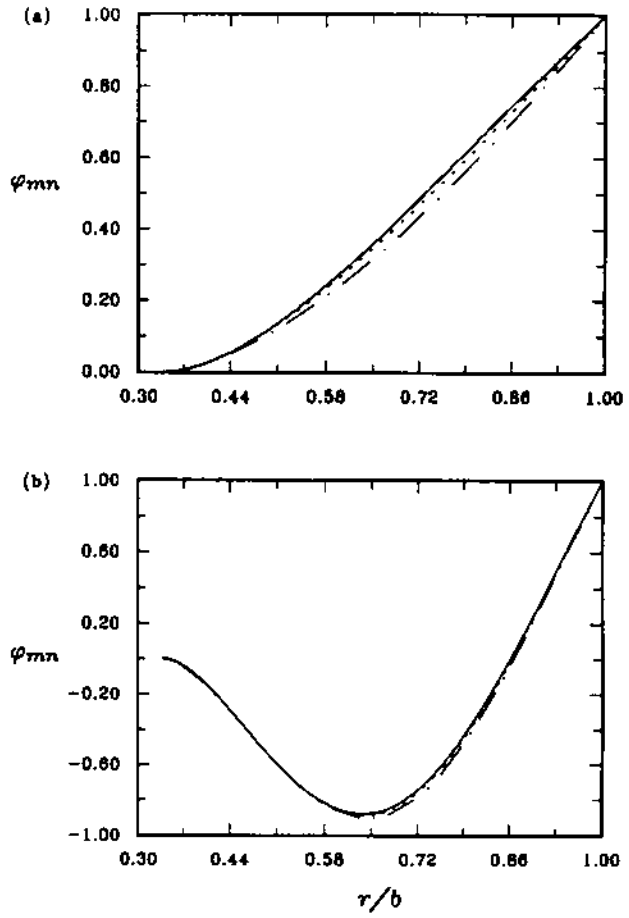

FIG. 3. Predicted vibration modes. Key: ——— (a) (0,1) mode, (b) (1,1) mode; — — — (a) (0,2) mode, (b) (1,2) mode; ----- (a) (0,3) mode, (b) (1,3) mode.

the complicated integrals involved by using numerical, analytical, or asymptotic expansion techniques.

Investigation of radiation characteristics of planar radiators vibrating in their elastic modes has been conducted both analytically and experimentally.[9–16] Holographs of near-field sound pressure of a clamped circular plate vibrating in its natural modes are presented in an early paper.[9] Predicted and measured near-field sound intensity flow of a clamped circular plate in resonant vibration are also available in Krishnappa and McDougall's study.[10] Theoretical prediction in their work is based on Rayleigh's integral and the finite-difference approximation, and measurements were carried out by using a two-microphone intensity probe. Levine and Leppington[11] analyzed modal radiated sound power by using an exact integral representation for frequencies above the modal coincidence. Asymptotic solutions for the radiation efficiency of a clamped circular plate vibrating at high frequency modes are derived. Similar analyses on beams and rectangular panels were performed by Levine[12] in an early paper. Williams[13] derived a power series representation of sound power in terms of the wave number for the planar radiator of arbitrary geometry. Others have performed related research on the sound radiation dealing with the effects of distributed load on rectangular plates,[14] internal damping and

viscous/thermal losses,[15] and arbitrary boundary conditions.[16]

As described in Sec. I, our polynomial approximation matches the exact modal function almost perfectly. Consequently, we can use the approximated modal functions to derive the formulation for radiated sound without losing any accuracy from the engineering viewpoint. The object here is to develop formulation for radiated sound from an annular disk by using the structural modal base. The modal radiation efficiency of a single stationary disk is formulated first to analyze acoustic characteristics of the disk vibrating in its rigid body modes or elastic deformation modes. Two specific methods, namely, the far-field approach and the impedance approach, are developed to formulate the modal radiated sound power Π_{mn}.

A. Far-field approach

This approach essentially employs the free-field Green's function and geometric far-field assumption to evaluate radiated sound. Sound pressure for Fig. 1 is given by employing the Raleigh's integral[13] and is represented by

$$P_{mn}(R,\theta,\phi)=\frac{j\omega_{mn}\rho_0}{2\pi}\int_0^{2\pi}\int_a^b \frac{\psi_{mn}(r,\varphi)e^{-jk_{mn}d}}{d}\,r\,dr\,d\varphi, \tag{11}$$

where $d=R-r\cos(\varphi-\phi)\sin\theta$ is the distance between the source and observation points. The approximated modal function, Eq. (7), is rewritten in terms of the dimensionless radial coordinate,

$$\psi_{mn}(r,\varphi)=\cos(n\varphi)\sum_{s=0}^{N}\bar{c}_{mn,s}\left(\frac{r}{b}\right)^s, \tag{12a}$$

$$\bar{c}_{mn,j}=\left(\frac{b}{a}\right)^j\sum_{\substack{i=j\\ i>2}}^{N}(-1)^{i+j}\frac{i!}{(i-j)!j!}a^i c_{mn,j}. \tag{12b}$$

With the geometric far-field assumption, $R\gg r$, the far-field modal sound pressure P_{mn} is obtained by substituting the approximated modal function, Eq. (12), into Eq. (11). It is expressed by

$$P_{mn}(R,\theta,\phi)=\frac{j^{n+1}e^{-jkR}\rho_0 c k_{mn}\cos(n\phi)}{R}\times\sum_{s=0}^{N}\bar{c}_{mn,s}\int_a^b r^{s+1}J_n(k_{mn}r\sin\theta)dr. \tag{13}$$

Since the far-field impedance is the characteristic impedance $\rho_0 c$, the modal sound power Π_{mn} is obtained by integrating the far-field sound intensity over a hemispherical surface in the far field. By expressing Bessel function of the first kind in terms of a power series, the modal sound power is represented in terms of a convergent power series of the modal wave number k_{mn}:

$$\Pi_{mn}=\frac{R^2}{2\rho_0 c}\int_0^{2\pi}\int_0^{\pi/2}P_{mn}(R,\phi,\theta)P_{mn}(R,\phi,\theta)^*\times\sin\theta\,d\theta\,d\phi$$

$$=\frac{\rho_0 c\pi b^2}{\epsilon_n}(k_{mn}b)^{2(n+1)}\sum_{s=0}^{\infty}A_{mn,s}(k_{mn}b)^{2s}, \tag{14a}$$

where

$$\epsilon_n=\begin{cases}1, & n=0,\\ 2, & \text{otherwise},\end{cases} \tag{14b}$$

$$A_{mn,s}=\frac{[(s+n)!]^2(-1)^s}{(2s+2n+1)!}\sum_{t_1,t_2=0}^{N}\bar{c}_{mn,t_1}\bar{c}_{mn,t_2}\times\sum_{q=0}^{s}\frac{(1-\alpha^{\lambda_1})(1-\alpha^{\lambda_2})}{q!(s-q)!(n+q)!(s+n-q)!\lambda_1\lambda_2}, \tag{14c}$$

$$\lambda_1=t_1+2q+n+2, \tag{14d}$$

$$\lambda_2=t_2+2(s-q)+n+2, \tag{14e}$$

$$\alpha=a/b. \tag{14f}$$

The symbol * denotes the complex conjugate of a function. The coefficients $A_{mn,s}$ of this power series representation are clearly the functions of the geometry of the disk. Since the radiated sound is represented in terms of a convergent series of the wave number, it is convenient to relax the accuracy of predictions and implement it in a computer code by limiting the number of terms included in the series. The corresponding reference power, which is defined as the acoustic power radiated from an analogous piston of the same area and the same averaged mean-square velocity in the translating mode, is given by

$$\Pi_{mn,\mathrm{ref}}=\frac{\rho_0 c\pi b^2}{\epsilon_n}\sum_{t_1,t_2=0}^{N}\bar{c}_{mn,t_1}\bar{c}_{mn,t_2}\frac{1-\alpha^{t_1+t_2+2}}{t_1+t_2+2}. \tag{15}$$

Consequently, the modal radiation efficiency σ_{mn} is

$$\sigma_{mn}=\Pi_{mn}/\Pi_{mn,\mathrm{ref}}. \tag{16}$$

B. Impedance approach

In this approach, the disk is discretized into sever concentric annuli and each annulus is assumed to have uniformly distributed velocity in the radial direction. Tl velocity distribution of the s-th annulus surface of $r_{o,s}$ ar $r_{i,s}$ as the outer and inner radii is

$$\psi_{mn,s}(\varphi)=\psi_{mn}(\bar{r}_s)\cos(n\varphi), \tag{17}$$

$$\bar{r}_s=(r_{o,s}+r_{i,s})/2. \tag{17}$$

The self-radiation impedance of a single annulus with ri body motion is available in the literature.[2–4,7] Using t concept, the self-radiation impedance of sth annulus gi the velocity distribution of Eq. (17) is[32]

$$Z_{mn,ss}=\frac{2\pi\rho_0 c k_{mn}}{\epsilon_n}\int_0^{k_{mn}}\frac{f_n^2(\xi)\xi\,d\xi}{\sqrt{k_{mn}^2-\xi^2}}, \tag{1}$$

$$f_n(\xi)=\int_{r_{i,s}}^{r_{o,s}}J_n(\xi r)r\,dr. \tag{1}$$

The final expansion is again represented in terms of a vergent series of the wave number and is given by

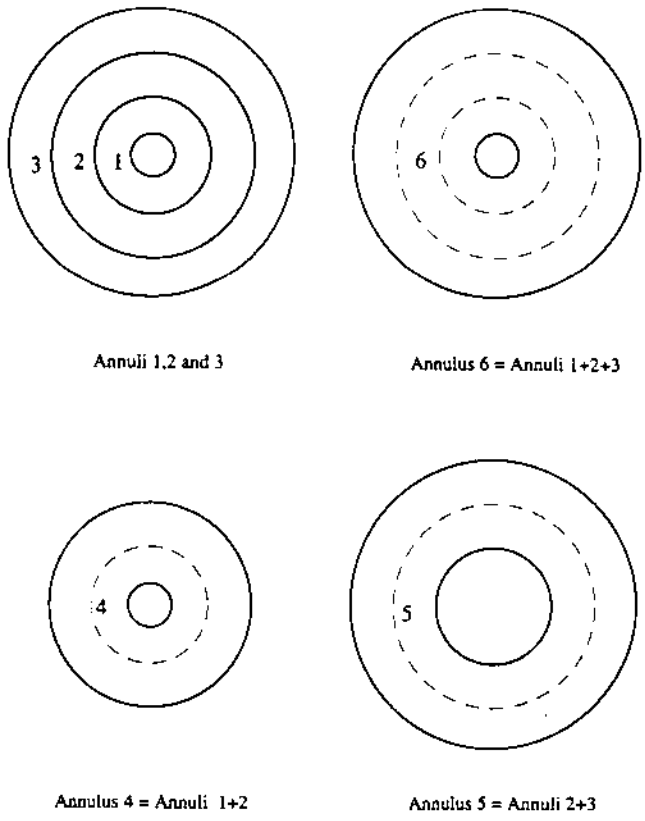

Annuli 1,2 and 3 — Annulus 6 = Annuli 1+2+3

Annulus 4 = Annuli 1+2 — Annulus 5 = Annuli 2+3

FIG. 4. Definition of annuli for the impedance approach used to calculate the mutual radiation impedance.

$$Z_{mn,ss}=\frac{\pi}{\epsilon_n}\rho_0 c(k_{mn}r_{o,s})^{2(n+1)}\sum_{t=0}^{\infty}B_t(k_{mn}r_{o,s})^{2s}, \quad (19a)$$

$$B_t=\frac{[(t+n)!]^2(-1)^t}{(2t+2n+1)!} \times\sum_{q=0}^{t}\frac{(1-\alpha_s^{\beta_1})(1-\alpha_s^{\beta_2})}{q!(t-q)!(n+q)!(t+n-q)!\beta_1\beta_2}, \quad (19b)$$

$$\beta_1=2q+n+2, \quad (19c)$$

$$\beta_2=2(t-q)+n+2, \quad (19d)$$

$$\alpha_s=r_{i,s}/r_{o,s}. \quad (19e)$$

Mutual-radiation impedance between two nonconsecutive concentric annuli is derived in terms of self-radiation impedances. Given three consecutive annuli (numbers 1, 2, and 3 in Fig. 4), the mutual-radiation impedance between 1 and 3 is

$$Z_{mn,13}=\tfrac{1}{2}(Z_{mn,66}+Z_{mn,22}-Z_{mn,55}-Z_{mn,44}), \quad (20)$$

where annulus 4 contains annuli 1 and 2, annulus 5 contains annuli 3 and 4, and annulus 6 consists of annuli 1, 2, and 3, as defined in Fig. 4. With the formulations of self and mutual radiation impedances, the sound power radiated from each annulus is formulated by

$$\Pi_{mn,s}=Z_{mn,ss}\psi_{mn}^2(\bar{r}_s)+\sum_{t=1,\,t\neq s}^{N_a}Z_{mn,st}\psi_{mn}(\bar{r}_s)\psi_{mn}(\bar{r}_t), \quad (21)$$

TABLE III. Predicted modal radiation efficiencies of a stationary disk.[a]

Modal index (m,n)	Natural frequency (Hz)	σ_{mn} Far-field approach	σ_{mn} Impedance approach	σ_{mn} BEMAP (Ref. 33)
(0,0)	604	$0.842E-1$	$0.842E-1$	$0.842E-1$
(0,1)	602	$0.272E-2$	$0.272E-2$	$0.272E-2$
(0,2)	713	$0.749E-4$	$0.749E-4$	$0.739E-4$
(0,3)	1120	$0.187E-4$	$0.187E-4$	$0.170E-4$
(0,4)	1820	$0.223E-4$	$0.222E-4$	$0.212E-4$
(0,5)	2750	$0.485E-4$	$0.484E-4$	$0.454E-4$
(0,6)	3870	$0.138E-3$	$0.138E-3$	$0.145E-3$
(0,7)	5180	$0.457E-3$	$0.456E-3$	$0.491E-3$
(0,8)	6670	$0.164E-2$	$0.163E-2$	$0.174E-2$
(0,9)	8330	$0.608E-2$	$0.606E-2$	$0.632E-2$
(1,0)	3890	0.330	0.329	0.335
(1,1)	4050	0.322	0.322	0.325
(1,2)	4540	0.111	0.112	0.112
(1,3)	5390	$0.403E-1$	$0.405E-1$	$0.400E-1$
(1,4)	6620	$0.281E-1$	$0.283E-1$	$0.274E-1$
(1,5)	8220	$0.452E-1$	$0.455E-1$	$0.433E-1$

[a] m, number of nodal circles; n, number of nodal diameters.

where N_a is the total number of annuli. The total modal sound radiated from the disk is then obtained by summing the power emitted by each annulus and is expressed by

$$\Pi_{mn}=\begin{bmatrix}\psi_{mn}(\bar{r}_1)\\ \psi_{mn}(\bar{r}_2)\\ \vdots\\ \psi_{mn}(\bar{r}_{N_a})\end{bmatrix}^T\begin{bmatrix}Z_{mn,11} & Z_{mn,12} & \cdots & Z_{mn,1N_a}\\ Z_{mn,21} & Z_{mn,22} & \cdots & Z_{mn,2N_a}\\ \vdots & \vdots & \ddots & \vdots\\ Z_{mn,N_a1} & Z_{mn,N_a2} & \cdots & Z_{mn,N_aN_a}\end{bmatrix} \times\begin{bmatrix}\psi_{mn}(\bar{r}_1)\\ \psi_{mn}(\bar{r}_2)\\ \vdots\\ \psi_{mn}(\bar{r}_{N_a})\end{bmatrix}. \quad (22)$$

The radiation efficiencies of selected vibration modes as predicted by both approaches are compared with numerical results yielded by a boundary element program BEMAP[33] in Table III. The annular disk was discretized into 30 concentric annuli and 48 quadratic elements were used in the boundary element model. Excellent agreement is found between the two analytical approaches. Analytical predictions match the numerical results very well for those modes which have a few nodal diameters. Apparently, as the number of nodal diameters is increased, more elements are required by the boundary element model to yield accurate results. Figure 5 illustrates the contribution of sound power from each annulus, normalized with respective to the area of the annulus for two axisymmetric modes.

The impedance approach yields the radiated sound power associated with each annulus. This information can be used in structure modification or active noise control studies of annular/circular type radiators. Nevertheless, the impedance approach is more complicated than the far-

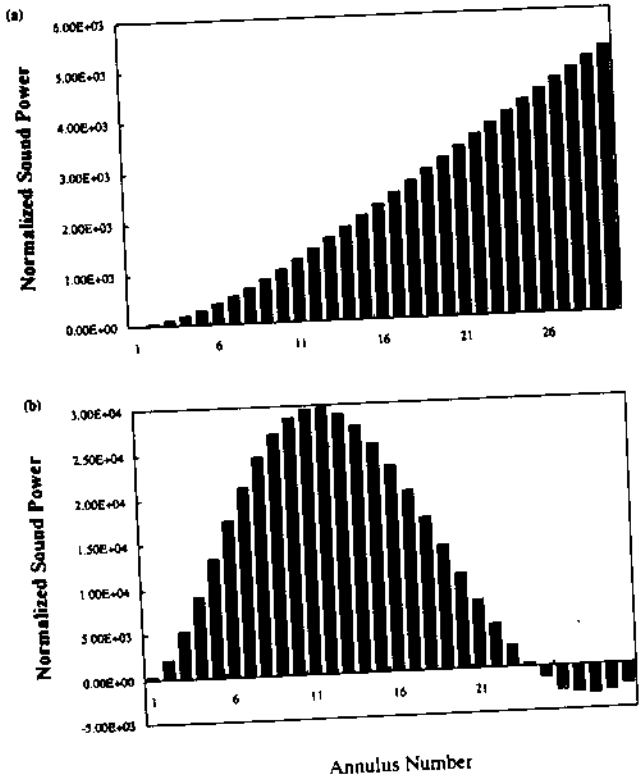

FIG. 5. Contribution to the normalized sound power from each annulus by using the impedance approach. (a) (0,0) mode. (b) (1,0) mode.

field approach which expresses the sound power in terms of a power series of the wave number. The latter method can be easily computer coded and this advantage becomes apparent for the multimodal case which will be discussed in Sec. III.

C. Rigid body modes

Two rigid body modes, namely, the rigid translating and rigid rocking modes, are also included. To distinguish them from the elastic modes, the radial modal index m is *intentionally* assigned the value -1 for these modes. The corresponding tangential modal index n (number of nodal diameters) is 0 for the rigid translating mode (classical piston radiator) and 1 for the rigid rocking mode, respectively. The radiation efficiency of these two rigid body modes can be derived directly by using either the far-field approach or the impedance approach. The normalized surface velocity functions are represented by

$$\psi_{-1,0}=1/\sqrt{(b^2-a^2)\pi}, \tag{23}$$

$$\psi_{-1,1}=[2/\sqrt{(b^4-a^4)\pi}]r\cos(\varphi). \tag{24}$$

Figure 6 shows the calculated radiation efficiencies of both modes for the example case.

III. MODAL COUPLING EFFECTS

If several structural modes are excited simultaneously, coupling effects between the acoustic field generated by different modes need to be included. Literature on this subject is very sparse and has considered only cases of one-dimensional beams.[17-19] For instance, Keltie and Peng[17] found that the coupling between two natural modes is as important as the individual mode when both natural frequencies are much lower than the excitation frequency. Cunefare[18,19] developed a quadratic expression for the radiation efficiency of a beam under multimodal excitation by using a far-field intensity integration technique. It has been shown that the minimization of radiation efficiency becomes essentially an eigenvalue type problem in a form identical to the Rayleigh's quotient employed in the discipline of vibrations.

A. Modal formulation

From the far-field formulation, it can be easily shown that nonzero sound power due to the coupled modes exists only when the coupled modes have the same number of nodal diameters. Assume that the disk is excited by a harmonic force of frequency ω and the velocity distribution can be expressed in terms of normalized elastic and rigid body modes ψ, so that

$$w=\eta^T\psi, \tag{25a}$$

$$\psi=[\psi_{-1,0}\quad \psi_{-1,1}\quad \psi_{00}\quad \psi_{01}\quad \cdots\quad \psi_{0n}\quad \psi_{10}\quad \psi_{11}\quad \cdots\quad \psi_{mn}]^T, \tag{25b}$$

$$\eta=[\eta_{-1,0}\quad \eta_{-1,1}\quad \eta_{00}\quad \eta_{01}\quad \cdots\quad \eta_{0n}\quad \eta_{10}\quad \eta_{11}\quad \cdots\quad \eta_{mn}]^T. \tag{25c}$$

Here, the elastic modes are grouped by the number of nodal circles, and the same number of natural modes are selected for each group. In addition to the rigid body modes, $(m+1)$ groups with $(n+1)$ natural modes in each one are included in the formulation. If some of the selected natural modes are not excited, the corresponding modal participating factors are numerically set to be zero. The far-field pressure is then expressed by

$$P=\eta^T\mathbf{P}, \tag{26a}$$

$$\mathbf{P}=\frac{jk\rho_0 c}{2\pi R}\int_0^{2\pi}\int_a^b \psi e^{-jkd_r}\,dr\,d\varphi. \tag{26b}$$

Consequently, the overall radiation efficiency expression is as follows, where $\mathbf{I}_n$ is an identity matrix of dimension n:

$$\sigma = \eta^H \Pi \eta / \tfrac{1}{2}\rho_0 c \eta^H G \eta, \tag{27a}$$

$$\Pi = \frac{R^2}{2\rho_0 c} \int_0^{2\pi} \int_0^{\pi/2} \mathbf{P}^H \mathbf{P} \sin\theta \, d\theta \, d\phi, \tag{27b}$$

$$\mathbf{G} = \int_0^{2\pi} \int_a^b \psi^T \psi r \, dr \, d\varphi = \begin{bmatrix} \mathbf{I}_2 & \mathbf{M}^T \\ \mathbf{M} & \mathbf{I}_{(m+1)} \end{bmatrix},$$

$$\mathbf{M}^T = \begin{bmatrix} \langle \psi_{-1,0}, \psi_{00} \rangle & 0 & 0 & \cdots & \langle \psi_{-1,0}, \psi_{m0} \rangle \\ 0 & \langle \psi_{-1,1}, \psi_{01} \rangle & 0 & \cdots & 0 \end{bmatrix} \quad \begin{matrix} 0 & 0 & \cdots & 0 \\ \langle \psi_{-1,1}, \psi_{m1} \rangle & 0 & \cdots & 0 \end{matrix}, \tag{27c}$$

$$\langle \psi_{m_1 n_1}, \psi_{m_2 n_2} \rangle = \int_0^{2\pi} \int_a^b \psi_{m_1 n_1} \psi_{m_2 n_2} r \, dr \, d\varphi. \tag{27d}$$

For an arbitrary plate, the modal sound power Π is a fully populated matrix whose elements need to be evaluated numerically. For the annular disk, it consists of $(m+2)$ by $(m+2)$ submatrices and is expressed by

$$\Pi = \begin{bmatrix} \Pi^{-1,-1} & \Pi^{-1,0} & \cdots & \Pi^{-1,m} \\ \Pi^{0,-1} & \Pi^{00} & \cdots & \Pi^{0m} \\ \vdots & \vdots & \ddots & \vdots \\ \Pi^{m,-1} & \Pi^{m0} & \cdots & \Pi^{mm} \end{bmatrix}, \tag{28a}$$

$$\Pi^{ij} = \begin{bmatrix} \Pi^{i0}_{j0} & \Pi^{i0}_{j1} & \cdots & \Pi^{i0}_{jn} \\ \Pi^{i1}_{j0} & \Pi^{i1}_{j1} & \cdots & \Pi^{i1}_{jn} \\ \vdots & \vdots & \ddots & \vdots \\ \Pi^{in}_{j0} & \Pi^{in}_{j1} & \cdots & \Pi^{in}_{jn} \end{bmatrix}, \tag{28b}$$

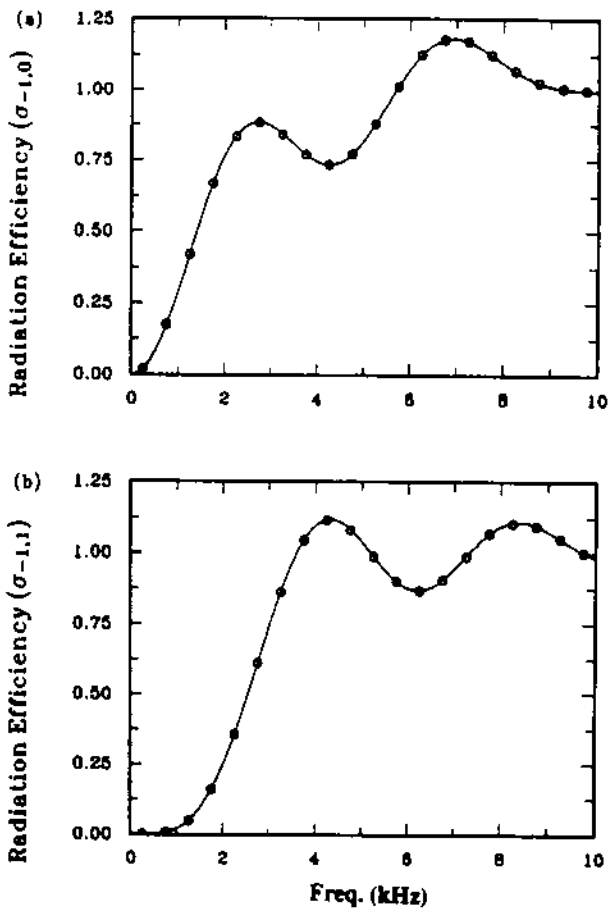

FIG. 6. Radiation efficiency for the rigid body modes of a single stationary disk; (a) translating piston mode, (b) rocking piston mode. Key: ———, analytical formulation; ○○○○, BEMAP program.

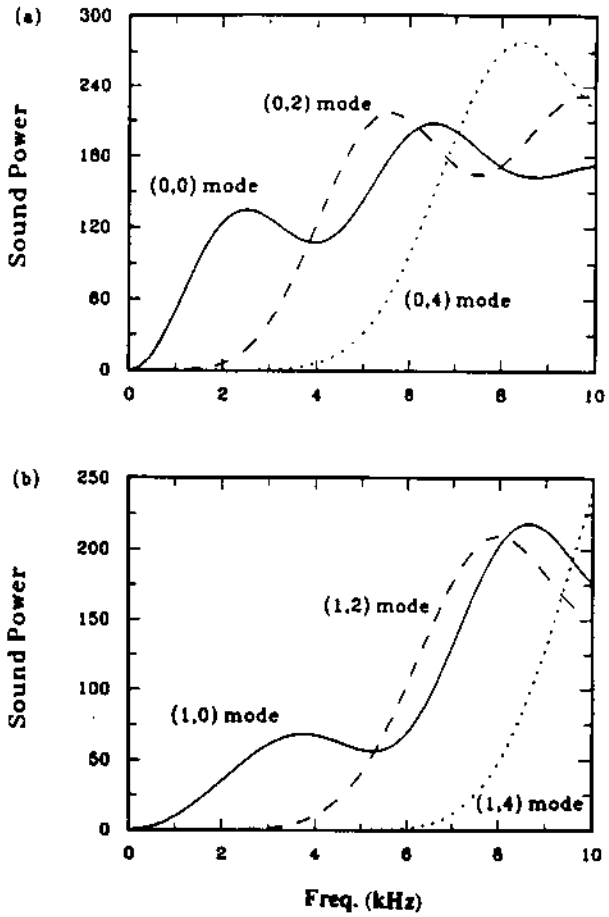

FIG. 7. Selected self-radiation terms of sound power for multimodal excitation. Key: ———, (a) (0,0) mode, (b) (1,0) mode; — — —, (a) (0,2) mode, (b) (1,2) mode; ----, (a) (0,4) mode, (b) (1,4) mode.

$$\Pi_{jn_2}^{in_1}=\frac{R^2}{2\rho_0 c}\int_0^{2\pi}\int_0^{\pi/2}P_{in_1}P_{jn_2}^{*}\sin\theta\,d\theta\,d\phi. \tag{28c}$$

It is evident from Eq. (28c) that only those modes that have the same number of nodal diameters, i.e., $n_1=n_2$, contribute to the radiated sound. Therefore, each submatrix Π^{ij} is a diagonal matrix (DIAG) expressed by

$$\Pi^{ij}=\begin{cases}\text{DIAG}[\Pi_{j0}^{i0}\quad\Pi_{j1}^{i1}\quad\cdots\quad\Pi_{jn}^{in}], & \text{for } i,j\neq -1,\\ \text{DIAG}[\Pi_{j0}^{i0}\quad\Pi_{j1}^{i1}\quad 0\quad\cdots\quad 0], & \text{for } i \text{ or } j=-1.\end{cases} \tag{29}$$

For $i=j$, the submatrices represent the sound power associated with the individual elastic or rigid body modes. Other submatrices are due to the modal coupling effects between different modes. Each element of these submatrices is formulated in terms of a wave-number power series as developed in the previous section. Figures 7–10 show selected self (single mode) and coupled (multiple mode) terms of the radiated sound power of the sample disk for sinusoidal excitation up to 10 kHz. From these results, it is observed that self-radiated sound power spectra associated with elastic modes that have the same number of nodal circles (index m) essential have the similar patterns, except that the humps shift to higher frequencies as the number of nodal diameters (index n) is increased. For the sound power associated with the modal coupling effect, similar phenomena are observed for selected natural modes, and all of them have positive contributions to the overall radiated sound power. However, if a higher number of n is included, the destructive interference, i.e., sound cancellation in the modal domain, may also exist.

Figure 11 shows typical results for the disk vibrating with the following surface velocity distribution:

$$\psi=[\psi_{00}\quad\psi_{01}\quad\psi_{02}\quad\psi_{10}\quad\psi_{11}\quad\psi_{12}]^T, \tag{30a}$$

$$\eta=[0.5\quad 1\quad 0.2\quad 0.3\quad 0.8\quad 0.4]^T. \tag{30b}$$

B. Harmonic force or moment excitation

The transverse motion of a computer disk can be excited by the sinusoidal axial force or bending moment due to a coupling between the bearing stiffness and structural impedance at the junction between casing cover and spindle shaft. For a concentrated harmonic force excitation of frequency ω, in the axial direction distributed along the inner edge of disk, the response of disk is a combination of the rigid translating mode and axisymmetric elastic modes. The transverse deformation of the disk is represented by

$$w=[\eta_{-1,0}\quad\eta_{00}\quad\cdots\quad\eta_{m0}]\times[\psi_{-1,0}\quad\psi_{00}\quad\cdots\quad\psi_{m,0}]^T. \tag{31}$$

Assuming that the amplitude of the rigid piston mode is equal to w_p, then the modal participating factors of elastic modes are obtained by using Eq. (1) and the normal mode expansion method. They are expressed by

$$\eta_{m0}=\frac{2\pi\omega^2 w_p}{(\omega_{m0}^2-\omega^2)\sqrt{(b^2-a^2)\pi}}\sum_{s=0}^{N}\bar{c}_{m0,s}b^{s+2}\frac{(1-\alpha^{s+2})}{(s+2)}. \tag{32}$$

The radiation efficiency is thus obtained by substituting Eq. (32) into Eqs. (27)–(29). Similarly, for a concentrated sinusoidal moment excitation at the center, only the rigid rocking mode $(-1,1)$ and the elastic modes with one nodal diameter $(m,1)$ are excited. The response of the disk is

$$w=[\eta_{-1,1}\quad\eta_{01}\quad\cdots\quad\eta_{m1}]\times[\psi_{-1,1}\quad\psi_{01}\quad\cdots\quad\psi_{m1}]^T. \tag{33}$$

Again, the participating factors of elastic modes are represented below in terms of the amplitude of the rigid rocking mode (w_r):

$$\eta_{m1}=\frac{2\pi\omega^2 w_r}{(\omega_{m1}^2-\omega^2)\sqrt{(b^4-a^4)\pi}}\sum_{s=0}^{N}\bar{c}_{m1,s}b^{s+3}\frac{(1-\alpha^{s+3})}{s+3}. \tag{34}$$

Figure 12 shows predicted radiation efficiency for excitation spectrum.

IV. EFFECT OF DISK ROTATION

The effect of source motion on the sound radiation from circular or annular plates is obviously of interest in many applications but literature on this topic deals primarily with aerodynamic sources.[20–22] Typically, sources are assumed to be either classical point sources (monopole, dipole, and quadrupole) or a combination of them to simplify the mathematical formulations.[23–25] Majority of approaches employ the far-field Green's function of a moving source evaluated at the retarded time. For instance, Lowson[23] extended Lighthill's[20] theory for a point force in uniform rectilinear motion into a general expression which takes into account the acceleration of source motion. Morfey and Tanna[24] employed Lowson's result to study the point force in a circular motion. Overall sound power is evaluated by calculating the autocorrelation of sound pressure. Levine and Leppington[25] used a different approach to derive an expression for the instantaneous sound power radiated by a point source in an arbitrary motion; the formula essentially is the same as the one yielded by Lowson's result. A point monopole–dipole combination is investigated to study interaction. For the moving surface, analysis is based on an extension to the Kirchhoff's formulation.[26–28] One way to apply the Kirchhoff's theory is to assume a hypothetical surface which replaces the surface of a moving radiator.[26,27] The sound field is the same as the real field outside the hypothetical surface but it is arbitrary inside. A generalized function theorem is then employed to represent the discontinuities across the hypothetical surface. The other approach includes the turbulence effects associated with the moving surface.[28]

A. Natural frequencies of a rotating disk

If the disk is rotating at Ω_r rad/s, the potential energy expression, Eq. (8), must be modified to include the additional potential energy ΔPE associated with a rotation-induced in-plane stress:[34]

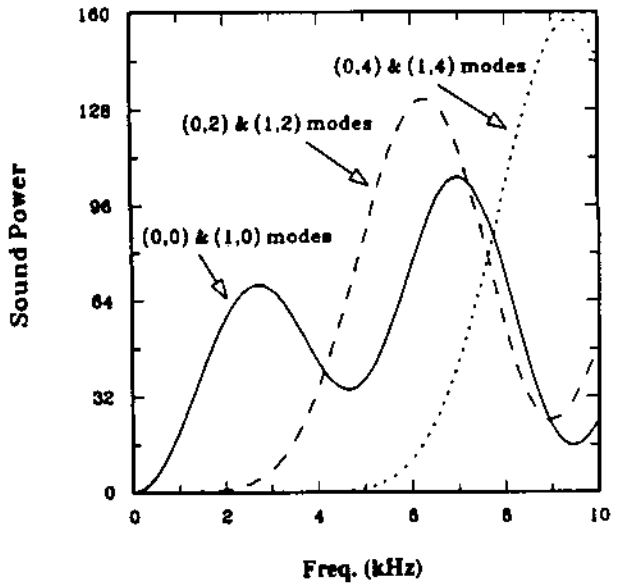

FIG. 8. Selected mutual radiation terms of sound power between elastic modes. Key: ———, (0,0) and (1,0) modes; — — —, (0,2) and (1,2) modes; ····· (0,4) and (1,4) modes.

$$\Delta \mathrm{PE}=\frac{1}{2}\left(\frac{3+\nu}{8}\right)\Omega_r^2\rho h\int_0^{2\pi}\int_a^b\left\{\left[\left[a^2+b^2-r^2-\left(\frac{ab}{r}\right)^2\right]\times\left(\frac{\partial w}{\partial r}\right)+\left[a^2+b^2-\frac{1+3\nu}{3+\nu}r^2+\left(\frac{ab}{r}\right)^2\right]\times\left(\frac{1}{r}\frac{\partial w}{\partial \varphi}\right)^2\right\}r\,dr\,d\varphi. \tag{35}$$

Consequently, the contribution of the in-plane stress to the coefficients of a set of linear equations given by Eq. (10) is derived as

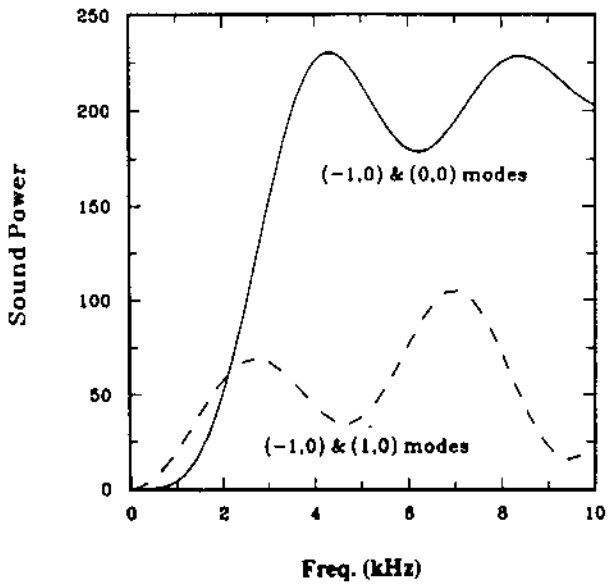

FIG. 9. Selected mutual radiation terms of sound power between rigid translating piston mode and elastic modes. Key: ———, (−1,0) and (0,0) modes; — — —, (−1,0) and (1,0) modes.

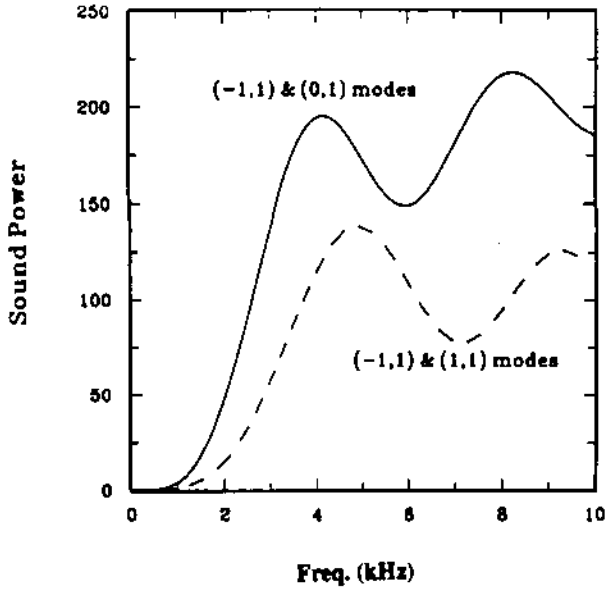

FIG. 10. Selected mutual radiation terms of sound power between rigid rocking mode and elastic modes. Key: ———, (−1,1) and (0,1) modes; — — —, (−1,−1) and (1,1) modes.

$$\Delta\Lambda_{ij}=\left(\frac{3+\nu}{8D}\right)\Omega_r^2\rho h\left[ij\left[(a^2+b^2)X_1^{i+j-2}-X_3^{i+j-2}-(ab)^2X_{-1}^{i+j-2}\right]+n^2\left((a^2+b^2)X_{-1}^{i+j}-\frac{1+3\nu}{3+\nu}X_1^{i+j}+(ab)^2X_{-3}^{i+j}\right)\right], \tag{36a}$$

$$X_3^l=X_3^{l+3}+3aX_3^{l+2}+3a^2X_3^{l+1}+a^3X_3^l. \tag{36b}$$

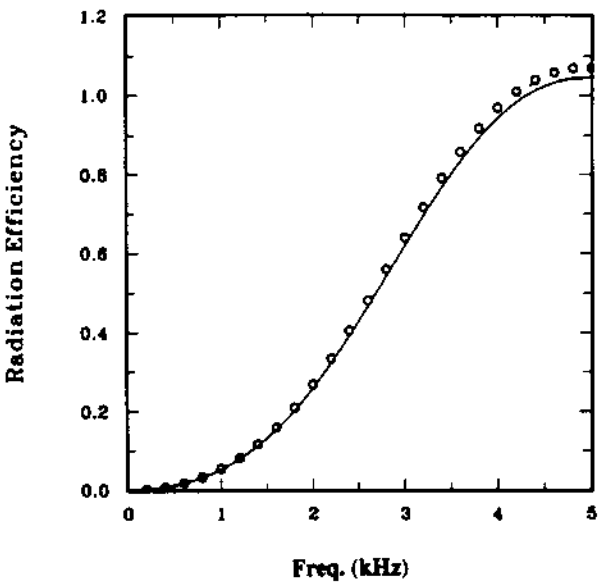

FIG. 11. Radiation efficiency for the multi-mode excitation. Key: ———, analytical formulation; ○○○○, BEMAP program.

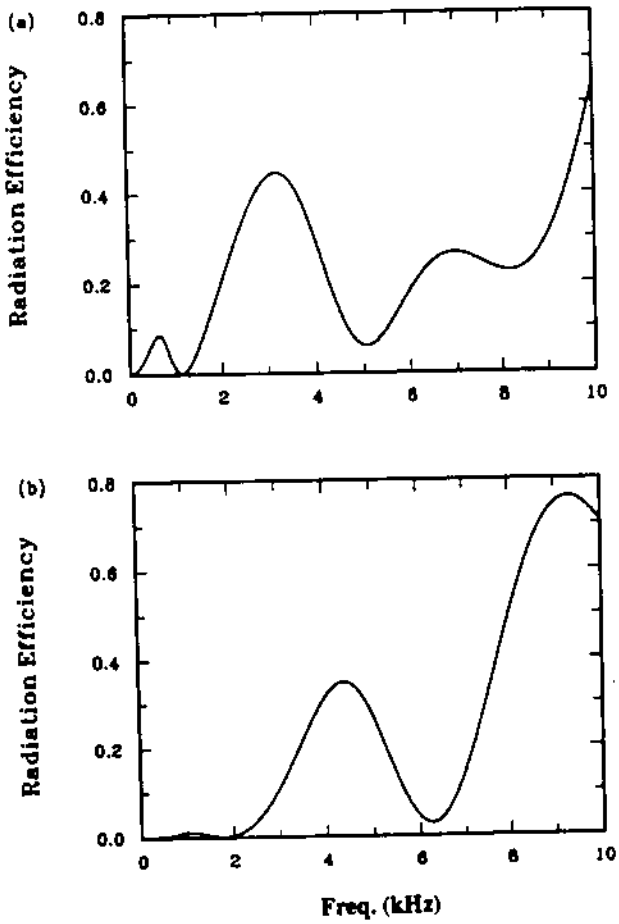

FIG. 12. Radiation efficiency of a disk under a concentric harmonic excitation; (a) axial force excitation, (b) moment excitation.

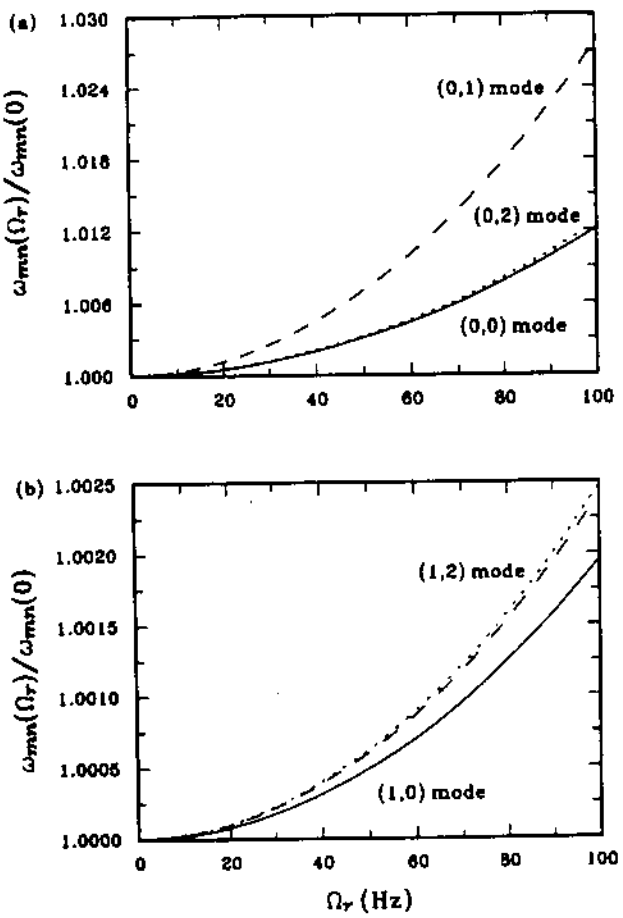

FIG. 13. Effect of disk rotation on the normalized natural frequency. Key: ———, (a) (0,0) mode, (b) (1,0) mode; — — —, (a) (0,1) mode, (b) (1,1) mode; ·····, (a) (0,2) mode, (b) (1,2) mode.

Selected natural frequencies of the rotating disk with the rotational speeds up to 100 Hz are shown in Fig. 13. It is seen that the increase of natural frequency is approximately proportional to Ω_r^2, which has also been observed by Ramaiah.[34]

B. Effect of rotation on modal radiation efficiency

To account for the rotational motion of sound source, an expression for the Green's function of a moving sound source is used instead of the stationary one in deriving the far-field sound pressure of the disk.[25] Integrating the Green's function over the surface of the disk, we obtain the following expression for sound pressure in the far-field:

$$P_{mn}(R,\theta,\phi,t)=\frac{\rho_0}{2\pi R}\int_0^{2\pi}\int_a^b\left[\left(\frac{\psi_{mn}}{(1-M_r)^2}+\frac{\psi_{mn}\dot{M}_r}{(1-M_r)^3}\right)r\,dr\,d\varphi\right], \tag{37}$$

where [ ]′ denotes evaluation at retarded time $t'=t-d/c$ and the M_r is the Mach number in the direction toward the observation position. For observation in the far field, it can be written by

$$M_r=(\Omega_r r/c)\sin\theta\sin(\phi-\varphi-\Omega_r t'). \tag{38}$$

By taking the Fourier transform on the sound pressure time history, the spectrum of pressure is

$$P_{mn}(R,\theta,\phi,\omega)=\int_0^\infty P_{mn}(R,\theta,\phi,t)e^{j\omega t}\,dt. \tag{39}$$

The relationship between the observation time t and the retarded time t' is

$$t'=t-(1/c)[R-r\cos(\phi-\varphi-\Omega_r t')\sin\theta], \tag{40}$$

$$dt=[1-M_r]'\,dt'. \tag{41}$$

The sound pressure is then evaluated by substituting Eqs. (37), (38), (40), and (41) into Eq. (39) and letting the reference frame rotate synchronously with the disk. Assuming the subsonic speed condition $\Omega_r b/c\ll 1$, we incorporate the following approximations in evaluating the integral equation:

$$(1-M_r)^{-1}\approx 1+M_r, \tag{42}$$

$$(1-M_r)^{-2}\approx 1+2M_r. \tag{43}$$

The final expression of sound pressure in the far field, as given below, is obtained after a tedious mathematical manipulation:

$$P_{mn}=\frac{(-j)^{n}\rho_0 c\pi}{2R}\sum_{s=0}^{\infty}\sum_{q=0}^{\infty}\bar{c}_{mn,q}\frac{(-1)^{s}(k_{mn}\sin\theta)^{2s+n}}{s!(s+n)!2^{2s+n}}\left|j\left\{2k_{mn}\cos(n\phi)\,Y_{2s+n+q+1}-k_{mn}\left(\frac{\Omega_r}{c}\right)\sin(n\phi)\right.\right.$$
$$\times\left(\frac{k_{mn}\sin^2\theta}{2(s+n+1)}\,Y_{2s+n+q+3}+\frac{2(s+n)}{k_{mn}}\,Y_{2s+n+q+1}\right)+\left(\frac{\Omega_r}{c}\right)^2\cos(n\phi)\left(\frac{k_{mn}\sin^2\theta}{2(s+n+1)}\,Y_{2s+n+q+3}\right.$$
$$\left.\left.-\frac{2(s+n)}{k_{mn}}\,Y_{2s+n+q+1}\right)\right\}+\left(\frac{\Omega_r}{c}\right)^3\sin(n\phi)\left(\frac{k_{mn}^2\sin^4\theta}{4(s+n+1)(s+n+2)}\,Y_{2s+n+q+5}\right.$$
$$\left.\left.-\frac{4(s+n)(s+n-1)}{k_{mn}^2}\,Y_{2s+n+q+1}\right)\right|, \tag{44a}$$

where

$$Y_t=\int_a^b r^t\,dr=\frac{b^{t+1}-a^{t+1}}{t+1}. \tag{44b}$$

Figure 14 shows normalized radiation efficiencies obtained by using the above expression and Eq. (14) derived early for the stationary case for rotational speed up to 100 Hz. Both expressions yield almost the same results. Therefore, the effect of source rotation on σ_{mn} can be ignored in this case for engineering purposes. An increase in modal radiation efficiency can however be taken into account simply by considering an increase in natural frequencies and the change of mode shapes without losing any accuracy. Figure 15 shows clearly a linear relationship between the normalized radiation efficiency and the square of the normalized speed $(\Omega_r/\omega_{mn})^2$. The following simple empirical equation for selected modes has been found for the sample case:

$$\frac{\sigma_{mn}(\Omega_r)}{\sigma_{mn}(0)}\approx 1+(2n-1)^2\left(\frac{\Omega_r}{\omega_{mn}}\right)^2 Q_m,$$

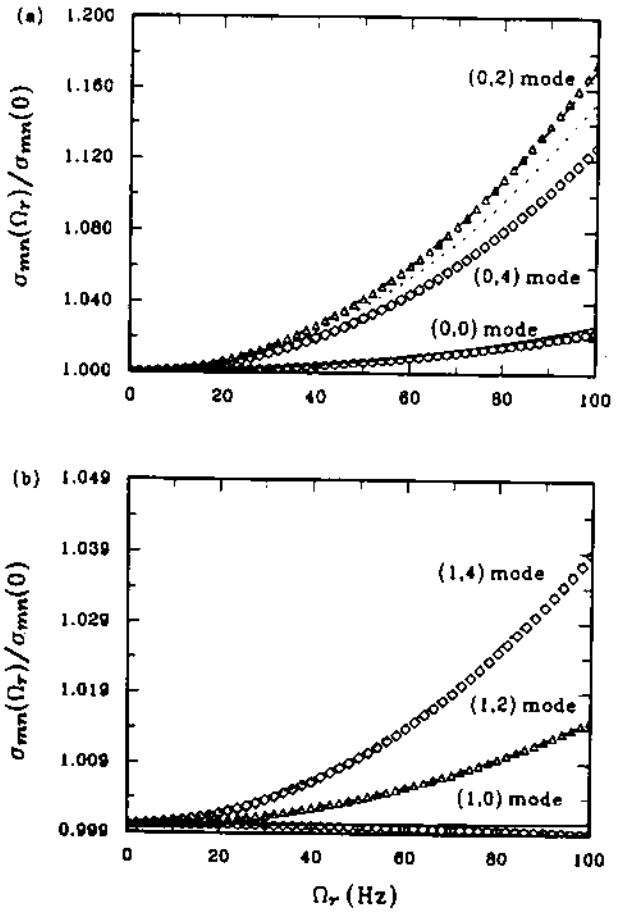

FIG. 14. Effect of disk rotation on the normalized modal radiation efficiency: empty symbols: formulation for stationary cases; solid line, formulation including source rotation effect. Key: ——— and ○○○○, (a) (0,0) mode, (b) (1,0) mode; — — — and ΔΔΔΔ, (a) (0,2) mode, (b) (1,2) mode; ----- and □□□□, (a) (0,4) mode, (b) (1,4) mode.

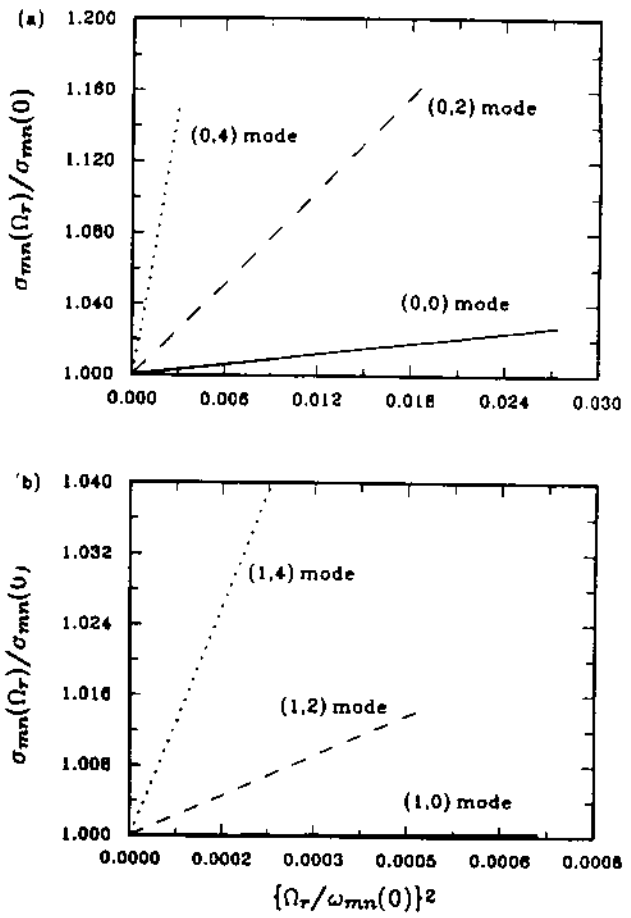

FIG. 15. Normalized modal radiation efficiency versus normalized rotational speed. Key: ———, (a) (0,0) mode, (b) (1,0) mode; — — —, (a) (0,2) mode, (b) (1,2) mode; -----, (a) (0,4) mode, (b) (1,4) mode.

TABLE IV. Radiation efficiency of a rotating disk at $\Omega_r/2\pi=72$ Hz.[a]

Modal index (m,n)	Natural frequency (Hz)	σ_{mn} at $\Omega_r/2\pi=72$ Hz: Rotating disk Eq. (44)	Stationary disk Eq. (14)	Approximate formulation Eq. (45)
(0,0)	608	$0.854E-1$	$0.853E-1$	$0.853E-1$
(0,1)	608	$0.278E-2$	$0.282E-2$	$0.275E-2$
(0,2)	724	$0.814E-4$	$0.815E-4$	$0.811E-4$
(0,3)	1130	$0.205E-4$	$0.203E-4$	$0.204E-4$
(0,4)	1830	$0.239E-4$	$0.237E-4$	$0.238E-4$
(0,5)	2760	$0.512E-4$	$0.508E-4$	$0.509E-4$
(0,6)	3880	$0.144E-3$	$0.143E-3$	$0.143E-3$
(0,7)	5190	$0.472E-3$	$0.470E-3$	$0.470E-3$
(0,8)	6680	$0.168E-2$	$0.168E-2$	$0.168E-2$
(0,9)	8340	$0.620E-2$	$0.619E-2$	$0.619E-2$
(1,0)	3890	0.330	0.329	0.330
(1,1)	4050	0.323	0.323	0.322
(1,2)	4540	0.112	0.112	0.112
(1,3)	5400	$0.410E-1$	$0.409E-1$	$0.409E-1$
(1,4)	6630	$0.287E-1$	$0.287E-1$	$0.286E-1$
(1,5)	8230	$0.463E-1$	$0.462E-1$	$0.462E-1$

[a] m, number of nodal circles; n, number of nodal diameters.

$$Q_m=\begin{cases}0.89, & \text{for } m=0,\\ 3.3272, & \text{for } m=1.\end{cases} \tag{45}$$

A quantitative comparison between analytical results and approximations for a disk rotating at 72 Hz, which is the running speed of the sample disk drive, is given in Table IV. It is observed that disk rotation has a more significant effect on the modal radiation efficiency. For instance, the maximum increases in natural frequency and modal radiation efficiency are 3% and 16%, respectively, for the sample problem with the rotational speeds up to 100 Hz, as shown in Figs. 13 and 14.

V. CONCLUSION

The proposed methodology has yielded new analytical formulations for modal radiation efficiencies of a computer disk. The modal base concept as developed in this study yields an efficient and direct method to predict the sound radiation of an annular disk radiator. Our formulations, which are expressed in terms of power series of the wave number, are convenient since they can be easily computer coded. This method can also be combined with vibratory energy calculations in order to develop a systematic narrow-band approach for calculating both structure-borne and radiated sounds.[35]

ACKNOWLEDGMENTS

The authors gratefully acknowledge the IBM Corporation for financial support of this work under its SUR program with D. Yeager and R. Bengal as project monitors. The permission of Spectronics, Inc. for the use of BEMAP software is also appreciated.

[1] G. M. L. Gladwell, "A note on the radiation from a circular piston in a plane wall," J. Sound Vib. **9**, 1–5 (1969).
[2] A. S. Merriweather, "Acoustic radiation impedance of a rigid annular ring vibrating in an infinite rigid baffle," J. Sound Vib. **10**, 369–379 (1969).
[3] W. Thompson, Jr., "The computation of self- and mutual-impedances for annular and elliptical piston using Bouwkamp's integral," J. Sound Vib. **17**, 221–233 (1971).
[4] C. J. Bouwkamp, "Numerical computation of the radiated impedance of a rigid annular ring vibrating in an infinite plane rigid baffle," J. Sound Vib. **17**, 499–508 (1971).
[5] F. P. Mechel, "Notes on the radiation impedance, especially of piston-like radiators," J. Sound Vib. **123**, 537–572 (1988).
[6] P. R. Stepanishen, "Impulse response and radiation impedance of an annular piston," J. Acoust. Soc. Am. **56**, 305–312 (1974).
[7] P. R. Stepanishen, "Evaluation of mutual radiation impedances between circular pistons by impulse response and asymptotic methods," J. Sound Vib. **59**, 221–235 (1978).
[8] M. Greenspan, "Piston radiator: some extensions of the theory," J. Acoust. Soc. Am. **65**, 608–621 (1979).
[9] C. H. Hansen and D. A. Bies, "Near field determination of the complex radiation efficiency and acoustic intensity distribution for a resonantly vibrating surface," J. Sound Vib. **62**, 93–110 (1979).
[10] G. Krishnappa and J. M. McDougall, "Sound intensity distribution and energy flow in the nearfield of a clamped circular plate," ASME Trans. J. Vib. Acoust. Stress Reliabil. Des. **111**, 465–471 (1989).
[11] H. Levine and F. G. Leppington, "A note on the acoustic power output of a circular plate," J. Sound Vib. **121**, 269–275 (1988).
[12] H. Levine, "On the short wave acoustic radiation from planar panels or beams of rectangular shape," J. Acoust. Soc. Am. **76**, 608–615 (1984).
[13] E. G. Williams, "A series expansion of the acoustic power radiated from planar sources," J. Acoust. Soc. Am. **73**, 1520–1524 (1983).
[14] M. C. Junger, "Pressure radiated by an infinite plate driven by distributed loads," J. Acoust. Soc. Am. **74**, 649–653 (1983).
[15] K. U. Ingard and A. Akay, "Acoustic radiation from bending waves of a plate," ASME Trans. J. Vib. Acoust. Stress Reliabil. Des. **109**, 75–81 (1987).
[16] A. Berry, J.-L. Cuyader, and J. Nicolas, "A general formulation for the sound radiation from rectangular, baffled plates with arbitrary boundary conditions," J. Acoust. Soc. Am. **88**, 2792–2802 (1990).
[17] R. F. Keltie and H. Peng, "The effects of modal coupling on the acoustic power radiation from panels," ASME Trans. J. Vib. Acoust. Stress Reliabil. Des. **109**, 48–53 (1987).
[18] K. A. Cunefare, "The minimum multimodal radiation efficiency of baffled finite beams," J. Acoust. Soc. Am. **90**, 2521–2529 (1991).
[19] K. A. Cunefare, "Effect of modal interaction on sound radiation from vibrating structure," AIAA J. **30**, 2819–2828 (1992).
[20] M. J. Lighthill, "Sound generated aerodynamically," Proc. R. Soc. London Ser. A **267**, 147–182 (1962).
[21] M. V. Lowson and J. B. Ollerhead, "A theoretical study of helicopter rotor noise," J. Sound Vib. **9**, 197–222 (1969).
[22] R. Mani, "A moving source problem relevant to jet noise," J. Sound Vib. **25**, 337–347 (1972).
[23] M. V. Lowson, "The sound field for singularities in motion," Proc. R. Soc. London Ser. A **286**, 559–572 (1965).
[24] C. L. Morfey and H. K. Tanna, "Sound radiation from a point force in circular motion," J. Sound Vib. **15**, 325–351 (1971).
[25] H. Levine and F. G. Leppington, "The acoustic power from moving and pulsating sphere," J. Sound Vib. **146**, 199–210 (1991).
[26] F. Farassat and M. K. Myers, "Extension of Kirchhoff's formula to radiation from moving surfaces," J. Sound Vib. **123**, 451–460 (1988).
[27] M. K. Myers and J. S. Hausmann, "On the application of the Kirchhoff formula for moving surfaces," J. Sound Vib. **139**, 174–178 (1990).
[28] X.-F. Wu and A. Akay, "Sound radiation from vibrating bodies in motion," J. Acoust. Soc. Am. **91**, 2544–2555 (1992).
[29] L. Meirovitch, *Analytical Methods in Vibration* (Macmillan, New York, 1967).
[30] C. W. Bert, "Application of a version of Rayleigh technique to prob-

lems of bars, beams, columns, membrane and plates," J. Sound Vib. **119**, 317–326 (1987).
[31] C. S. Kim, P. G. Young, and S. M. Dickinson, "On the flexural vibration of rectangular plates approached by using simple polynomials in the Rayleigh–Ritz method," J. Sound Vib. **143**, 379–394 (1990).
[32] E. Skudrzyk, *Foundations of Acoustics* (Springer-Verlag, New York, 1971).
[33] A. F. Seybert and T. W. Wu, *User's Manual: Computer Program BEMAP* (Spectronics, Inc., Lexington, KY, 1989).
[34] G. K. Ramaiah, "Natural frequencies of spinning annular plates," J. Sound Vib. **74**, 303–310 (1981).
[35] J. E. Farstad, M.-r. Lee, and R. Singh, "Analysis of structure-borne and radiated sound using component modal bases," Appl. Acoust. (in press).